

Low-Area Ratio, Thrust-Augmenting Ejectors

RICHARD B FANCHER*

Aerospace Research Laboratories, Wright-Patterson Air Force Base, Ohio

The thrust augmentation, lift augmentation, and noise reduction characteristics of compact ejectors make them potentially attractive for propulsion lift systems; however, in the past, poor thrust augmentation results have negated the other benefits. A synthesis of an ejector's internal flow phenomena developed in this paper indicates that improved mixing and diffusion can significantly increase thrust augmentation. Experiments with an ejector employing a "hypermixing" primary nozzle confirm the analytical model's augmentation predictions and show reasonable agreement with other predicted flow characteristics. The two-dimensional primary nozzle has its slot-shaped exit throat divided into alternating segments that impart left and right deflections to the primary flow to accelerate mixing. The results indicate that a properly designed ejector should give a thrust augmentation ratio near $1.075 + 0.025(A_3/A_0)$, for $5 < A_3/A_0 < 14$, where A_3/A_0 is the ratio of the ejector's exit area to the primary nozzle area.

Nomenclature

| | |
|----------------|---|
| A | = area |
| $FWHV$ | = nozzle wake full width at half velocity |
| L | = length; over-all $L = L_M + L_D$ |
| \dot{m} | = mass flow rate |
| P, Q | = static and dynamic pressures ($Q = \rho V^2/2$) |
| T | = temperature |
| u, V | = inlet velocity ratio (V_1/V_0) and velocity |
| W | = diffuser entrance width = constant mixing duct width, where $A = A_2$ |
| x | = inlet area ratio; $x \equiv A_1/A_0 = (A_2/A_0) - 1$ |
| η | = efficiency |
| θ | = diffuser half angle |
| λ, ξ | = coflowing coefficient and loss coefficient |
| ρ, τ | = density and wall shearing stress |
| ϕ | = thrust augmentation ratio, Eq. (1) |
| Ψ^* | = skewness factor, Eq. (7) |

Subscripts

| | |
|--------------|---|
| D, I, M, N | = diffuser, inlet, mixing duct, and nozzle |
| or, tr, W | = orifice, transfer, and wetted |
| 0 | = primary nozzle exit |
| 1 | = secondary at primary nozzle exit |
| 2 | = end of mixing section and beginning of diffuser |
| 3 | = diffuser exit |

Superscripts

| | |
|-----|---------------------|
| () | = freejet condition |
|-----|---------------------|

Introduction

EJECTORS are potentially attractive to V/STOL use, because they are thrust augmentors, and they can be installed in an aerodynamic lifting body to create external characteristics which greatly augment aerodynamic lift.^{1,2,3} With acoustic lining, they may also provide the means to realize a low noise, high-lift device.⁴ To obtain reasonable thrust loading and to fit an ejector into an airframe, one desires a low ratio of secondary area to primary area A_1/A_0 , herein called the inlet area ratio, as well as a short length. However, until just recently, compact ejectors have shown dismal thrust perform-

ance, probably because the loss mechanisms and the mixing process were not understood. In this paper, a simplistic one-dimensional analytical development is extended to provide a more comprehensive model which synthesizes many of the internal flow phenomena. Then, an ejector experiment is described and its results are compared with the model's predictions.

Analytical Model Development

Thrust augmentation is produced by forcing a jet to mix with and entrain secondary fluid in a confined region, thereby, increasing the momentum efflux above that of a similar freejet. Thrust augmentation ratio is the ratio of the ejector's exit thrust to a reference thrust. Different investigators have used different reference thrusts; we use herein the isentropic thrust obtained by expanding to ambient pressure the same primary mass flow from the same primary reservoir pressure. Thus, the thrust augmentation ratio is (Fig. 1)

$$\phi = (\dot{m}_2/\dot{m}_0)(V_2/V_0)V_0/V_0' \quad (1)$$

where V_0' is the velocity that would be obtained if the primary fluid were exiting into ambient pressure. Assuming a constant-area mixing duct with isentropic, incompressible and one-dimensional flow, and using the Bernoulli, continuity, and momentum equations, the following relationships evolve

$$\dot{m}_2/\dot{m}_0 = 1 + ux \quad V_2/V_0 = (1 + ux)/(1 + x) \quad (2)$$

$$V_0/V_0' = (1 - u^2)^{-1/2} \quad (3)$$

where

$$u = V_1/V_0 = [(2x)^{1/2}(1 + x) - 2x]/(1 + x^2) \quad (4)$$

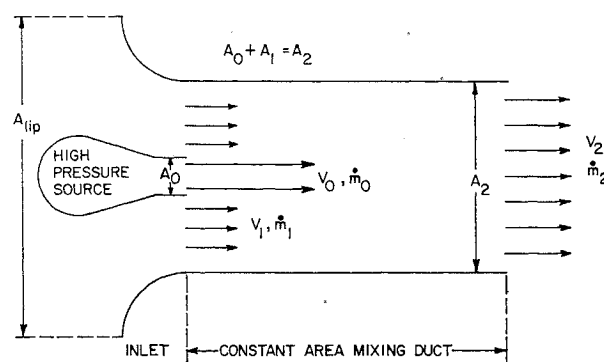


Fig. 1 Simple ejector schematic.

Presented as Paper 71-576 at the AIAA 4th Fluid and Plasma Dynamics Conference, Palo Alto, Calif., on June 21-23, 1971; submitted April 28, 1971; revision received November 17, 1971.

Index categories: Subsonic and Supersonic Air Breathing Propulsion; Jets, Wakes and Viscid-Inviscid Flow Interactions; Nozzle and Channel Flow.

* Research Engineer; presently Planning Engineer, Pacific Gas and Electric.

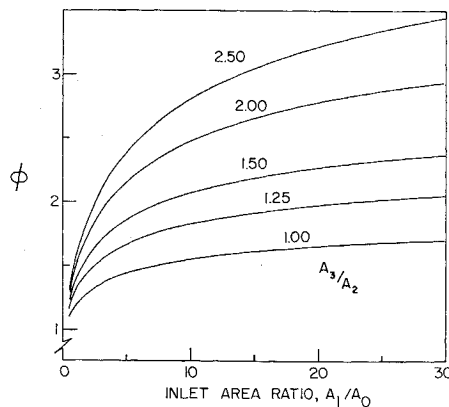


Fig. 2 Potential augmentation with an exit diffuser of area ratio A_3/A_2 .

In this case, ϕ is a strictly monotonic function for $x > 0$, increasing from 1 for $x = 0$ to 1.5 for $x = 14$, and it is asymptotic to 2 for large x . Diffusion of the mixed flow at station 2 results in higher ϕ . Figure 2 shows the potential thrust augmentation, where A_3 is the diffuser exit area.

Flow Losses

The performance potentials in Fig. 2 are rapidly diminished as diffuser efficiency,

$$\eta_D = 2(P_3 - P_2)/\rho(V_2^2 - V_3^2) \quad (5)$$

decreases. The geometric characteristics of two-dimensional diffusers are often described by two of the following three parameters: divergence half-angle θ , side-length/entrance-width ratio L_D/W , and area ratio A_3/A_2 . Kline has shown that in the case of two-dimensional, low L_D/W , rectangular diffusers, θ is higher for maximum pressure recovery than for maximum efficiency.⁵ Several investigators have reported that for ejectors with short diffusers, maximum ϕ is realized at θ 's between those for maximum efficiency and maximum pressure recovery.⁶⁻⁹ This observation, which can be analytically verified, shows that an optimized, constrained ejector requires a balance between pressure recovery, which increases entrained secondary flow, and efficiency, which conserves kinetic energy. Optimum η_D appears best characterized as a linear function of $\sin^2 2\theta$ (Fig. 3).¹⁰⁻¹⁴ The data points presented are only those which identify a locus of maximum performance. The solid

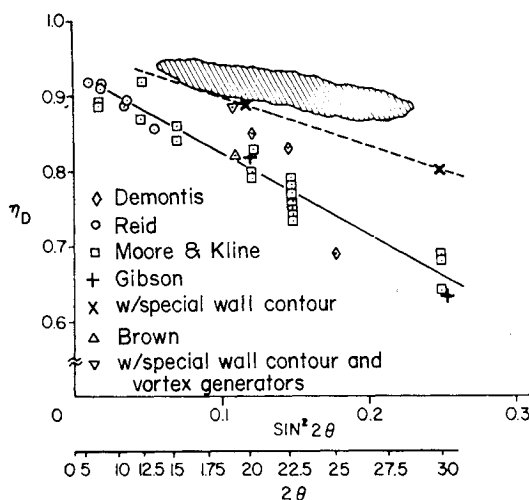


Fig. 3 Rectangular diffuser data.

line relates to straight-wall diffusers. Gibson²⁰ and Brown¹⁴ have reported that more efficient diffusion is possible with a trumpet-shaped wall. The dashed line corresponds to such diffusers. The hatched area represents diffuser efficiencies deduced from recent ejector experiments conducted at ARL.⁶ Some characteristics which may have caused this high performance are high turbulence and vorticity, boundary-layer energization, and low L/W 's. Unfortunately, except for the work of Demontis,¹⁰ there are no diffuser data for $L_D/W < 5$ and $\theta > 5^\circ$; for compact ejectors this is precisely the area of interest.

Rapid mixing requires primary nozzles of unconventional shapes and reduced hydraulic diameters. These characteristics decrease the velocity efficiency V_0/V_0' , which in turn decreases ϕ by the same factor. Additionally, the primary nozzles obstruct the secondary flow and generate drag losses. The secondary inlet passage should reach its minimum cross section at the injection plane. For well-designed inlets having $A_{1ip}/A_1 > 1.3$, the inlet $\Delta P/Q$ loss can be estimated from skin-friction drag.¹⁵ For the constant-area mixing duct, the skin friction is of the order, $\Delta P/Q \approx 0.01(L_M/D_{HM})$, where D_{HM} is the hydraulic diameter of the mixing duct. Aside from this friction loss, little attention has been directed toward the confined mixing phenomena found in ejectors.

Mixing

Although not explicitly stated, the simplified ejector analysis contained a kinetic energy loss associated with mixing. The energy transfer efficiency, $\eta_{tr} = \dot{m}_3 V_3^2 / \dot{m}_0 (V_0')^2$ is related to the entrained velocity ratio ($u = V_1/V_0$), since the following relationship holds for an ejector with no other losses

$$\eta_{tr} + (1 - u)^2 \approx 1 \quad (6)$$

Therefore, high-transfer efficiencies are obtained when the secondary velocity is a high percentage of the primary. It follows from Eq. (4) that η_{tr} is only possible in low-inlet, area-ratio (low x) ejectors. This is important, since high η_{tr} probably is desirable in propulsion-lift systems.

A unit of mass leaving a jet mixes with the surrounding fluid while diffusing energy and momentum in a direction normal to its flow axis. The mixing rate is often indicated by measuring gross changes in the jet such as the spreading rate. When a jet exits into a parallel coflowing stream, experiments have shown that the spreading rate is reduced by a factor λ that is a function of u . Several functions have been suggested, none of which fits all the data. Abramovich suggested the factor $\lambda = (1 - u)/(1 + u)$,¹⁶ which serves reasonably well. Unfortunately, the very characteristic which increases η_{tr} also lengthens the mixing distance, since from Eq. (6), together with the λ equation to the first order, $\lambda + \eta_{tr} \approx 1$. In case of low-area ratio ejectors with moderate diffusion, the coflowing effect reduces the spreading rate several times below that of a corresponding freejet.

The diminished spreading rate caused by the coflowing effect adequately describes ejector mixing until the jet wake impinges on either another wake (multiple jets are sometimes used) or the mixing chamber wall. At this stage, the mixing may not be sufficiently complete for good augmentation or diffusion, and, therefore, further mixing might be required. The postmerging characteristics of adjacent jets are not well known. However, the resultant velocity profile usually is at least as smooth as the superimposed profiles of individual jets. For the wall-impingement case, Abramovich suggested¹⁶ that the profile shape is similar to that of an unrestricted wake truncated to the mixing duct width as depicted in Fig. 4. The velocity profile shape is given by V_1 plus the shape of the jet without a coflowing stream when its wake is expanded to the same width. When the unrestricted jet wake is greater than the mixing duct width (region C), only the shape within the duct wall is included.

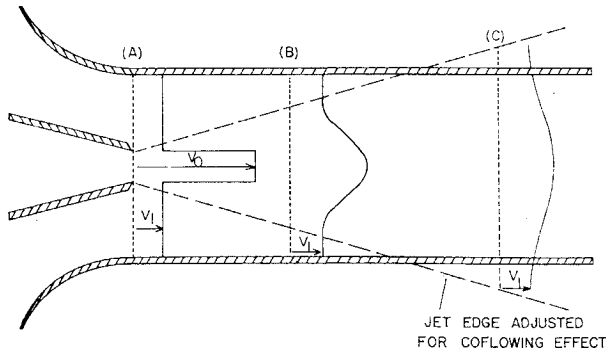


FIG. 4 Velocity profile model.

Fig. 4 Velocity profile model.

Model Synthesis

Nonuniform flows violate the one-dimensional assumption. However, if the nonuniformity is small it can be corrected for by a flow skewness parameter which relates impulse to average velocity. The skewness factor at any station i is

$$\Psi_i = \left[\int_{A_i} v_i^2 \frac{dA_i}{A_i} \right] / \left[\int_{A_i} v_i \frac{dA_i}{A_i} \right]^2 \quad (7)$$

This parameter is used to incorporate an effect of partially mixed flow into ejector analysis. If the shape of the velocity profile is specified by the coflowing effect, the jet's static characteristic, and a postimpingement model, Ψ_2 can be computed from continuity.

Incorporating the losses discussed into the momentum equation applied to the constant-area mixing duct section, we obtain

$$\dot{m}_1 V_1 + \dot{m}_0 V_0 + P_1(A_1 + A_0) = \Psi_2 \dot{m}_2 V_2 + (P_2 + Q_2 \xi_M) A_2 \quad (8)$$

where

$$P_2 = P_1 + (1 + \xi_i) Q_1 - \eta_D [1 - (A_2/A_3)^2] \quad (9)$$

is derived from the diffuser and inlet characteristics. The skin-friction loss coefficients for the inlet (ξ_i) and mixing duct (ξ_M) are defined as

$$\xi_i = \tau A_{W1}/Q_1 A_1; \quad \xi_M = \tau A_{WM}/Q_2 A_2 \quad (10)$$

The entrained velocity ratio u is found by the simultaneous solution of Eqs. (7-10) with the continuity equation. The thrust augmentation ratio is then

$$\phi = \eta_N (A_2/A_3) (1 + ux)^2 / (1 + x)(1 - u^2)^{1/2} \quad (11)$$

where η_N is the velocity efficiency of the primary nozzle.

From Eq. (8) we see that ϕ would increase if the skewness factor Ψ_2 or the mixing-duct, skin-friction loss ξ_M could be decreased. However, Ψ_2 decreases as the completeness of mixing increases; whereas, ξ_M increases as the mixing duct length L_M increases. Therefore, one wants to increase the mixing rate to achieve a low Ψ_2 in a shorter mixing duct. In an ejector of fixed over-all length L a shorter mixing duct also makes possible the benefit of a longer, more efficient diffuser. Figure 5 reveals the sensitivity of ϕ to L_M/W for ejectors with small over-all length-to-width ratios (L/W).

Clearly, the rewards of decreasing L_M are great. Such a decrease can be effected by either a decrease in the required spreading distance or an increase in the spreading rate of the jet wake. The former is possible up to the point where inlet blockage and additional viscous losses in both the primary and secondary cancel the benefits accrued from the reduced mixing distance. Increasing the wake spreading rate (hypermixing) offers interesting possibilities provided that the associated

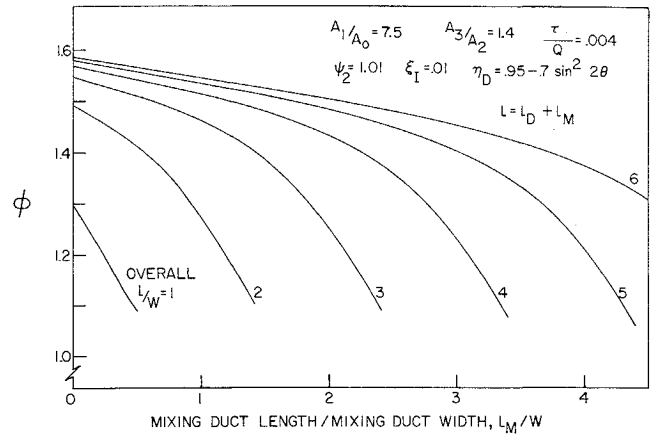


Fig. 5 The effect of mixing length.

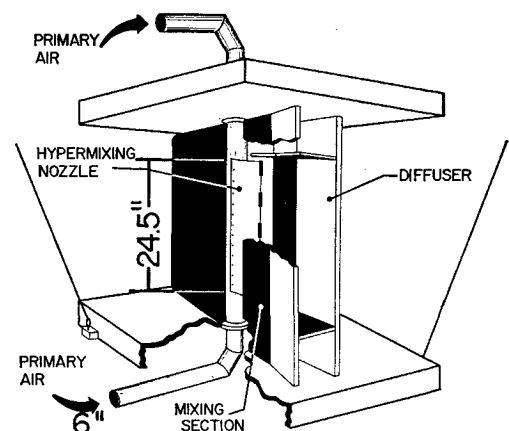
losses are small; a successful application of this idea is a key foundation of the ejector results presented in this paper.

Efficient diffusion is also necessary for high-thrust augmentation. For example with $x=10$ and $A_3/A_2=2$, ϕ is increased by 18% if η_D is increased from 85% to 95%.

Experimental Setup and Static Nozzle Performance

The experiments were conducted on an ejector designed to achieve high augmentation at $3 \leq A_1/A_0 \leq 10$. The schematic in Fig. 6 shows the 6 in.-diam cylinder which both holds the primary nozzle and supplies it with high-pressure air. The 5 ft-long cylinder is sandwiched between two horizontal surfaces which support the other ejector components. The apparatus hangs from four flexible cables.

The vertically oriented, adjustable walls form the ejector's shroud; consisting of the inlet, mixing duct, and diffuser. These were constructed by stretching 0.016 in. aluminum sheet across a series of rigid but adjustable bars. Each wall can be positioned independently; therefore, a large number of geometric configurations are possible. Figure 7 shows a scaled-cross-sectional view showing the wall shape used in most of the experiments; A_1/A_0 is varied by adjusting W ; the diffuser ratio is also variable. A unique feature is the "hypermixing" primary nozzle which is segmented into 24 elements $1\frac{1}{2}$ in.-long. Each element gives its exiting mass a velocity component normal to both the nozzle's major axis and the flow axis; the direction of this lateral velocity component alternates from element to element. This exit geometry was spawned from one of many geometries studies for their mixing and efficiency characteristics.¹⁷

Fig. 6 Schematic of ejector ($\frac{3}{4}$ view from rear).

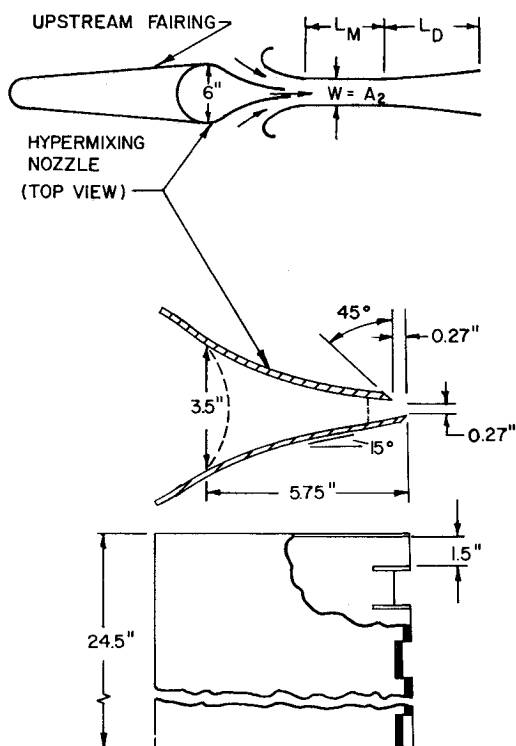


Fig. 7 Ejector cross section and details of hypermixing nozzle.

The force measurement was made with a dead-weight-calibrated, fixed load cell contacting the hanging ejector, which otherwise was free to move along the force axis. The total pressure and temperature measured just upstream of the primary nozzle determined the theoretical isentropic velocity V_o' . The mass flow \dot{m}_o was measured with a flat plate orifice. The static pressure upstream of the orifice (P_{or}), the pressure drop across the orifice (ΔP) and the orifice temperature (T_{or}) were measured.

The mass flow rate \dot{m}_o was determined by using the orifice as a relative measuring device. Using the same instrumentation, a mass flow calibration was obtained by the following method. An efficient contoured circular nozzle was installed in place of the hypermixing primary nozzle. Two different nozzles with exit areas straddling that of the primary nozzle were tested, and 65 data points were generated over a range of mass flows. A linear regression analysis of the nozzle's thrust divided by its isentropic velocity as a function of $(P_{or}\Delta P/T_{or})^{1/2}$ showed the correlation accuracy to be 0.9983 with a 0.06347 lb_m/sec standard estimate of error; this error equals 1.4% of the mean \dot{m}_o . The 90% predictive confidence band was $\pm 2.3\%$ of the mean.

The secondary flow was surveyed at the plane of primary injection with a direction-insensitive static pressure probe. The exit was surveyed with an averaging total pressure probe which measured the average pressure on a line parallel to the nozzle's major axis as the probe moved in the direction of the minor axis.¹⁸ It contained 41 half-in.-spaced, total pressure probes with a common reservoir. Total-pressure surveys were also made at the exit and inside the mixing duct with a Kiel probe.

The hypermixing nozzle was tested without a coflowing secondary with the objective of determining four characteristics: the wake spreading rate, the wake shape, the velocity efficiency and the nozzle exit area. The full width at half velocity, $FWHV$ (see Fig. 8), was used to characterize the nozzle-wake spreading rate. This was obtained by superimposing two Kiel probe profiles taken downstream of adjacent nozzle elements. Using this method the $FWHV$ was identical to that obtained from the averaging probe. The

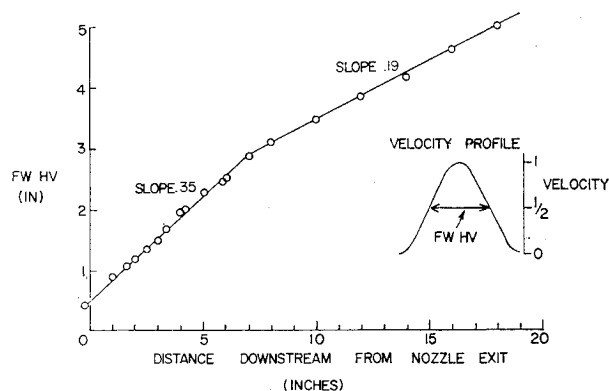


Fig. 8 Jet spreading rate.

results of these measurements (Fig. 8) revealed that the nozzle has almost double the normal planar jet spreading rate during its initial stage. After reaching 7 in. downstream, the spreading rate changes markedly and approaches that of a two-dimensional planar jet.¹⁹

The wake profiles obtained with the averaging probe were used to determine the wake shape. These surveys showed a displaced cosine shape between $-\pi$ and $+\pi$ corresponded almost identically with the velocity profile. There is no physical significance motivating this choice, but a shape characteristic is needed to predict skewness in the ejector model.

The nozzle thrust performance tests showed that the velocity efficiency was approximately 96% compared to the circular nozzles. Since a planar slot nozzle of this type would have an efficiency of about 98.5%, the cost of the nozzle's rapid mixing rate is about 2.5% in velocity efficiency.

The nozzle's unconventional exit made a direct measurement of A_o difficult and of questionable accuracy. Using ejector operating characteristics to determine A_o is hazardous, because the primary working fluid aspires into a mixing region of reduced static pressure. To circumvent this problem, A_o was determined from the incompressible relationship $F = 2\eta_N^2 \Delta P A_o$ and the thrust performance data of the nozzle alone. These experiments showed $A_o \approx 12.6 \text{ in.}^2$.

Ejector Performance and Its Comparison with Theory

The ejector was tested at inlet area ratios of 4.0, 6.5, and 8.6 with various diffuser settings. The typical experiment consisted of measurements taken at four primary Mach numbers, $M \approx 0.45, 0.55, 0.63$, and 0.70 . The results were insensitive to M as would be expected; therefore, the average thrust augmentation of each configuration is presented in Fig. 9. The pressure surveys showed that V_1 and V_3 were generally very uniform when measured with these highly time-damped devices. Table 1 compares measured V ratios to the values derived from the measured ϕ 's. (All numbers in Table 1 were computed to three decimal places and then rounded off to two.) At high-diffuser ratios, the augmentation decrease corresponds with unfavorable characteristics observed in the diffuser's

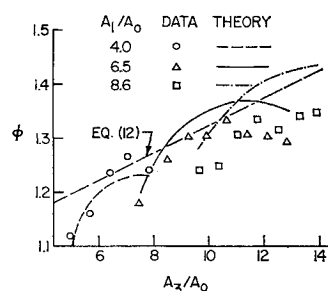


Fig. 9 Thrust augmentation and recommended approximation Eq. (12).

Table 1 Measured and predicted thrust augmentation (ϕ) and velocity ratios

| A_1/A_0 | A_3/A_2 | Average ϕ | | V_1/V_0 | | V_3/V_0 | |
|-----------|-----------|----------------|-------------|-----------|-------------------|-----------|-------------------|
| | | Meas. | Model pred. | Meas. | From meas. ϕ | Meas. | From meas. ϕ |
| 4.0 | 1.00 | 1.12 | 1.08 | 0.28 | 0.34 | 0.49 | 0.47 |
| | 1.14 | 1.16 | 1.18 | 0.34 | 0.38 | 0.46 | 0.44 |
| | 1.29 | 1.24 | 1.21 | 0.40 | 0.43 | 0.45 | 0.43 |
| | 1.43 | 1.27 | 1.22 | 0.42 | 0.47 | 0.42 | 0.40 |
| | 1.57 | 1.24 | 1.23 | 0.47 | 0.49 | 0.42 | 0.38 |
| 6.5 | 1.00 | 1.18 | 1.19 | 0.29 | 0.30 | 0.41 | 0.40 |
| | 1.14 | 1.26 | 1.30 | 0.32 | 0.35 | 0.38 | 0.38 |
| | 1.24 | 1.30 | 1.33 | 0.36 | 0.37 | 0.37 | 0.37 |
| | 1.43 | 1.33 | 1.36 | 0.40 | 0.41 | 0.36 | 0.34 |
| | 1.52 | 1.31 | 1.37 | 0.41 | 0.42 | 0.35 | 0.33 |
| | 1.62 | 1.30 | 1.36 | 0.42 | 0.44 | 0.34 | 0.32 |
| | 1.71 | 1.29 | 1.35 | 0.43 | 0.45 | 0.33 | 0.31 |
| 8.6 | 1.00 | 1.24 | 1.26 | 0.27 | 0.28 | 0.35 | 0.36 |
| | 1.07 | 1.24 | 1.33 | 0.30 | 0.30 | 0.36 | 0.35 |
| | 1.15 | 1.30 | 1.37 | 0.31 | 0.32 | 0.35 | 0.34 |
| | 1.22 | 1.33 | 1.40 | 0.33 | 0.34 | 0.34 | 0.33 |
| | 1.30 | 1.31 | 1.42 | 0.33 | 0.35 | 0.34 | 0.32 |
| | 1.38 | 1.34 | 1.43 | 0.36 | 0.37 | 0.34 | 0.31 |
| | 1.44 | 1.35 | 1.43 | 0.35 | 0.38 | 0.31 | 0.31 |

exit velocity profile. In these cases, the velocity peaked in the center and the flow was noticeably more unsteady. These stall characteristics were especially evident in the $A_1/A_0 = 8.6$ ejector.

The measured values of V_1/V_0 generally were lower than computed from ϕ . This may be attributed to the difficulty of defining the injection plane's position and to the fact that A_1 was slightly higher than the assumption that $A_1 = A_2 - A_0$. In contrast, the V_3/V_0 measurements were high; this may have been caused by the flow's unsteadiness, which will increase pressure probe readings.

In all tests, the flow remained attached to the endwalls, the minor ends of the ejector shroud. In many ejectors, it has been observed that the endwalls will stall and reverse flow, especially at high-diffuser angles. In this experiment, the primary flow attached to the endwalls soon after injection thereby preventing separation.

The ejector with $A_1/A_0 = 6.5$ and $A_3/A_2 = 1.43$ was investigated in more detail to ascertain the effects of higher primary Mach number and changes in geometry. The primary M was increased to 0.94, the limit of the air supply system. This test revealed no change in ϕ within the M range of 0.45 to 0.94. In other tests, the nozzle was positioned off center, causing an unbalanced inlet. The decreases in ϕ caused by inlet splits of 34/66, 14/86, and 0.100 were 2%, 10%, and 28%, respectively. In further tests, the shroud was positioned such that its axis was at an angle with the nozzle's center-line. With a 14/86 inlet split, ϕ increased by 3% as this angle was changed from 0 to 20°; ϕ then remained almost constant as the angle was increased up to 60°, where a physical limitation prevented larger angles. Exit pressure profiles showed that the exit velocity remained uniform as angle increased.

Figure 10 shows that the ejector's characteristics compared quite well with the model's predictions, for which it was assumed that $\tau/Q = 0.003$, the $FWHV$ was reduced by $\lambda = (1 - u)/(1 + u)$, the static nozzle's minor axis velocity profile was a displaced cosine curve between $-\pi$ and π , the primary nozzle velocity efficiency was 96%, the diffuser efficiency was given by $\eta_D = 0.95 - 0.6 \sin^2 2\theta$ for the ejectors with A_1/A_0 of 4.0 and 6.5, and $\eta_D = 0.95 - 0.8 \sin^2 2\theta$ for A_1/A_0 of 8.6. The lower η_D was used for the higher inlet area ratio because the nozzle spreading distance was quite large, giving a poor inlet velocity characteristic for the diffuser.

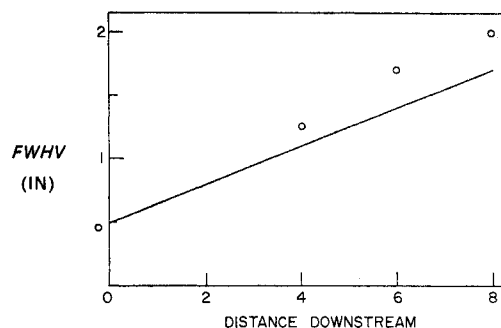


Fig. 10 Jet spreading rate in a coflowing stream.

Based on these results, the following equation, represented by the long-dashed line in Fig. 9, is recommended for rough approximation of achievable ϕ

$$\phi = 1.075 + 0.025 A_3/A_0 \quad (5 \leq A_3/A_0 \leq 14) \quad (12)$$

The jet mixing characteristics were examined in the $A_1/A_0 = 6.5$, $A_3/A_2 = 1.43$ ejector configuration. Total-pressure measurements showed that the jet spread at a rate greater than the coflowing adjusted static rate (see Fig. 10). With the mixing duct length extended to 11 in., pressure profiles showed that the assumed truncated velocity profile was a good description. Thus, this aspect of the model also appears to be satisfactory. The major remaining source of uncertainty is an adequate description of diffuser performance for $L_D/W > 5$ and $\theta > 5^\circ$.

Concluding Remarks

The improved analytical model for ejectors presented here is not perfect but is a step forward. It indicates that if the objective is high thrust augmentation, rapid mixing and efficient diffusion are necessary. An awareness of these requirements had led to the development of a hypermixing nozzle and an increased interest in diffuser efficiency. The thrust augmentation achieved experimentally, and the improved high understanding of ejector mechanics, increase the possibility that ejectors may be useful in STOL and V/STOL propulsion systems. If the effectiveness of powered aerodynamic lift increases with higher thrust augmentation, then these results suggest that ejectors may generate very favorable lift characteristics.

References

- Quinn, B., "A Wind Tunnel Investigation of the Forces Acting on an Ejector in Flight," ARL 70-0141, Dec. 1970, Aerospace Research Labs, Wright-Patterson Air Force Base, Ohio.
- Whittle, D. C., "The Augmentor Wing Research Program Past Present and Future," AIAA Paper 67-741, Los Angeles, Calif., 1967.
- Thornhill, W. J., "A Wind Tunnel Study of Forces Generated by an Ejector in a Free Stream," M.S. thesis, 1969, Air Force Institute of Technology, Wright-Patterson Air Force Base, Ohio.
- Kramer, J. J., et al., "Noise Reduction," SP-259, Nov. 1970, NASA.
- Kline, S. J., "On the Nature of Stall," *Journal of Basic Engineering*, Vol. 81, Series D, No. 3, Sept. 1959, pp. 305-320.
- Fancher, R. B., "A Compact Thrust Augmenting Ejector Experiment," ARL 70-0137, Aug. 1970, Aerospace Research Labs, Wright-Patterson Air Force Base, Ohio.
- Johnson, J. K., Jr., Shumpert, P. K., and Sutton, J. K., "Steady Flow Ejector Research Program," AD 263-180, Sept. 1961, Lockheed Aircraft Corp., Marietta, Ga.
- Alperin, M., Harris, G. L., and Smith, C. A., "An Experimental Investigation of New Concepts in Ejector Thrust Augmentation for V/STOL," AFFDL-TR-69-52, June 1969, Flight Dynamics Research Corp., Burbank, Calif.

⁹ Scott, W. J., "Experimental Thrust Augmentation of a Variable Geometry, Two-Dimensional, Coanda Wall Jet Ejector," LR-34, Jan. 1964, National Research Lab., Ottawa, Canada.

¹⁰ Demontis, J., "Recherches sur l'influence de l'angle d'ouverture d'un ajutage divergent sur l'écoulement à deux dimensions de l'air à travers cet ajutage," *Publication Sciences et Technologie du Ministère de l'air*, No. 87, 1936, Paris, France.

¹¹ Reid, E. G., "Performance Characteristics of Plane-Wall Two-Dimensional Diffusers," TN-2888, 1953, NACA.

¹² Moore, C. A., Jr. and Kline, S. J., "Some Effects of Vanes and Turbulence in Two-Dimensional Wide Angle Subsonic Diffusers," TN-4080, June 1958, NACA.

¹³ Patterson, G. N., "Modern Diffuser Design," *Aircraft Engineering*, Vol. 10, No. 115, Sept. 1938, pp. 267-273.

¹⁴ Brown, C. A. et al., "Subsonic Diffusers Designed Integrally with Vortex Generators," *Journal of Aircraft*, Vol. 5, No. 3, May-June 1968, pp. 221-229.

¹⁵ Blackaby, J. R. and Watson, E. C., "An Experimental Invest-

igation at Low Speeds of the Effect of Lip Shape on the Drag and Pressure Recovery of a Nose Inlet in a Body of Revolution," TN-3170, April 1954, NACA.

¹⁶ Abramovich, G. N., *The Theory of Turbulent Jets*, The MIT Press, Cambridge, Mass., 1963, p. 183 and p. 634.

¹⁷ Eastlake, C. N. II, "The Macroscopic Characteristics of Some Subsonic Nozzles and the Three-Dimensional Turbulent Jets They Produce," ARL 71-0058, April 1971, Systems Research Lab., Dayton, Ohio.

¹⁸ Silverstein, A. and Katzoff, S., "A Simplified Method for Determining Wing Profile Drag in Flight," *Journal of the Aeronautical Sciences*, Vol. 7, No. 7 May 1940, pp. 295-301.

¹⁹ Bradbury, L. J. S., "Simple Expressions for the Spread of Turbulent Jets," *The Aeronautical Quarterly*, Vol. 18, Part 2, May 1967, pp. 133-142.

²⁰ Gibson, A. H., "On the Resistance to Flow of Water Through Pipes or Passages Having Divergent Boundaries," *Transactions of the Royal Society Edinburgh*, Vol. 48, No. 5, 1913, pp. 97-116.

MARCH 1972

J. AIRCRAFT

VOL. 9, NO. 3

V/STOL Certification

JAMES F. RUDOLPH*

Federal Aviation Administration, Washington, D. C.

The new generation of Vertical/Short Takeoff and Landing (V/STOL) aircraft has many novel features which are not covered by the existing aircraft airworthiness standards. This has made it necessary for the Federal Aviation Administration (FAA), together with industry, to develop standards specifically oriented toward powered lift aircraft. These tentative standards have been released to the aviation community and are intended for trial application in new Short Takeoff and Landing (STOL) type certification projects. In addition to airworthiness certification standards, the FAA is also involved in the planning and development of the entire STOL system including air traffic control techniques, navigation and guidance equipment, and intercity STOL ports. Through the cooperation of the various government agencies and the aircraft industry, an important new element in our air transportation system is emerging.

V/STOL Certification

FOR many years there has been interest in aircraft which are capable of taking off and landing vertically or in short distances. As a result of this interest, back in 1966 a special government/industry advisory committee to the FAA Administrator recommended the formulation of tentative standards for emerging categories of aircraft. They further proposed that these tentative standards, once developed, be tried on for size, so to speak, in trial application prior to actual formal adoption. In that same year, the Vertical Lift Council of the Aerospace Industries Association (AIA) similarly recognized the need for VTOL and STOL standards and urged their development by mid-1968. The AIA volunteered to get the effort moving by formulating a working group, drawn from aircraft companies involved in the design of VTOL and STOL aircraft, for the purpose of preparing a first cut at the tentative standards. The FAA welcomed industry's offer and a program was established to ensure that all interested parties would be given an opportunity to make an input to the tentative standards.

Upon receipt of the AIA draft standards, they were reviewed by the FAA offices which would ultimately be charged with their implementation. Meetings were held with the AIA working group to ensure mutual understanding, and subsequently the public was invited to participate in reviewing and commenting on the draft tentative standards at a government/industry meeting in April 1968. After consideration of all the inputs received, the FAA in July 1968 issued the document titled "Tentative Airworthiness Standards for Verticraft/Powered Lift Transport Category Aircraft"—more commonly known as the "YELLOW BOOK." It was agreed at the time of the 1968 conference that the FAA would periodically review the standards with the aviation community for updating purposes. Such a meeting was held in April of 1970. The "YELLOW BOOK" was revised and distributed to the aviation community in Oct. 1970. I might mention that there was a slight change in the title of the document—the new one being "Tentative Airworthiness Standards for Powered Lift Transport Category Aircraft." The word "verticraft" was deleted since verticraft is only one form of a powered lift aircraft.

The purpose of the "YELLOW BOOK" is to present tentative airworthiness standards for study, trial application, and comment during the design and development of VTOL and STOL transport category aircraft. The tentative standards are not regulations and are not a formal notice of proposed rule making. Pending the adoption of regulations

Received September 1, 1971. Presented as Canadian Aeronautics and Space Institute Paper 72/21 at the 12th Anglo-American Aeronautical Conference, Calgary, Alberta, Canada, July 7-9, 1971.

*Director, Flight Standards Service.